Author Manuscript

Author Manuscript

Author Manuscript

Author Manuscript

HHS Public Access

Author manuscript

Mitochondrion. Author manuscript; available in PMC 2020 July 01.

Published in final edited form as:

Mitochondrion. 2019 July ; 47: 256–265. doi:10.1016/j.mito.2018.12.005.

Splitting the functions of Rim2, a mitochondrial iron/pyrimidine carrier

Simon A. B. Knight[a], **Heeyong Yoon**[a], **Ashutosh K. Pandey**[b], **Jayashree Pain**[b], **Debkumar Pain**[b], and **Andrew Dancis**[a,*]

[a]Department of Medicine, Division of Hematology-Oncology, Perelman School of Medicine, University of Pennsylvania, Philadelphia, Pennsylvania 19104, USA

[b]Department of Pharmacology, Physiology, and Neuroscience, New Jersey Medical School, Rutgers University, Newark, New Jersey 07103, USA

Abstract

Rim2 is an unusual mitochondrial carrier protein capable of transporting both iron and pyrimidine nucleotides. Here we characterize two point mutations generated in the predicted substrate-binding site, finding that they yield disparate effects on iron and pyrimidine transport. The Rim2 (E248A) mutant was deficient in mitochondrial iron transport activity. By contrast, the Rim2 (K299A) mutant specifically abrogated pyrimidine nucleotide transport and exchange, while leaving iron transport activity largely unaffected. Strikingly, E248A preserved TTP/TTP homo exchange but interfered with TTP/TMP hetero exchange, perhaps because proton coupling was dependent on the E248 acidic residue. Rim2-dependent iron transport was unaffected by pyrimidine nucleotides. Rim2-dependent pyrimidine transport was competed by Zn^{2+} but not by Fe^{2+}, Fe^{3+} or Cu^{2+}. The iron and pyrimidine nucleotide transport processes displayed different salt requirements; pyrimidine transport was dependent on the salt content of the buffer whereas iron transport was salt independent. In mitochondria containing Rim2 (E248A), iron proteins were decreased, including aconitase (Fe-S), pyruvate dehydrogenase (lipoic acid containing) and cytochrome *c* (heme protein). Additionally, the rate of Fe-S cluster synthesis in isolated and intact mitochondria was decreased compared with the K299A mutant, consistent with the impairment of iron-dependent functions in that mutant. In summary, mitochondrial iron transport and pyrimidine transport by Rim2 occur separately and independently. Rim2 could be a bifunctional carrier protein.

*Corresponding author at: Andrew Dancis: Department of Medicine, Division of Hematology-Oncology, Perelman School of Medicine, University of Pennsylvania, Philadelphia, PA 19104.

Author contributions: Simon Knight and Heeyong Yoon carried out the iron and nucleotide transport experiments, western blots and aconitase assays. Simon Knight also performed the genetic experiments, contributed to experimental design and paper writing. Jayashree Pain and Ashutosh K. Pandey performed Fe-S cluster loading and aconitase activity assays. Debkumar Pain designed experiments and wrote the paper. Andrew Dancis conceived the study, designed experiments and wrote the paper.

Conflict of interest: The authors declare that they have no conflicts of interest with the contents of this article.

Publisher's Disclaimer: This is a PDF file of an unedited manuscript that has been accepted for publication. As a service to our customers we are providing this early version of the manuscript. The manuscript will undergo copyediting, typesetting, and review of the resulting proof before it is published in its final citable form. Please note that during the production process errors may be discovered which could affect the content, and all legal disclaimers that apply to the journal pertain.

Author Manuscript Author Manuscript Author Manuscript Author Manuscript

Keywords

Yeast; mitochondria; iron; heme; iron-sulfur clusters; pyrimidine; mitochondrial carrier protein

1. Introduction

Iron is an essential metal for almost all organisms, required for Fe-S clusters, heme and diiron cofactors (1). Mitochondria contain the preponderance of iron in cells (2). They house a complete and functional Fe-S cluster assembly machinery, and thus are able to make these cofactors when supplied with ferrous iron and the amino acid cysteine as the source of sulfur (3). Likewise, mitochondria are the location of ferrochelatase, the final enzyme in the biosynthetic pathway responsible for insertion of iron into porphyrin to make heme (4). It is apparent that mitochondria must possess iron transporter(s) able to move iron from the outside (cytoplasmic face) to the interior (matrix face) of the inner membrane. The task of these transporter(s) must be accomplished without disrupting membrane potential across the inner membrane of mitochondria, because this is essential to oxidative phosphorylation. The only proteins purported to perform this function belong to the mitochondrial carrier family (MCF) and include Mrs3 and Mrs4 in the yeast *S. cerevisiae* (5–10). Mitoferrin 1 and 2 are the human orthologs (11, 12). Mrs3 and Mrs4 are redundant with each other, such that single deletions show minimal phenotypes. Even the double deletion yeast mutant shows a mild growth phenotype, although iron starvation produced during growth in low iron media renders the defect more severe (9). Based on this phenotype and the essential nature of iron delivery into mitochondria, the existence of additional iron transporters was anticipated, and Rim2, also a mitochondrial carrier protein, was shown to have mitochondrial iron transport activity (13).

Rim2 was first identified and linked to trace metal metabolism by a number of yeast genetic screens. In one screen, high copy expression of Rim2 was able to correct the splicing defect for the mitochondrial genes *COB* (cytochrome *b*) and *COXI* (cytochrome *c* oxidase subunit 1) resulting from *MRS2* deletion (14). Since Mrs2 is a magnesium transporter, it was proposed that Rim2 might bring extra magnesium or other trace metals into mitochondria, thereby facilitating RNA splicing (14). A second genetic screen involved deletion of *CCC1,* the vacuolar iron importer, thereby resulting in high cytoplasmic iron levels and sensitivity of cells to iron exposure. This iron sensitivity could be rescued by overexpression of Mrs3, Mrs4 or Rim2, suggesting that iron transport into mitochondria by any one of these three carrier proteins could relieve cytoplasmic iron overload and mitigate iron toxicity (15). A third screen was a synthetic lethal sectoring screen with Δ*mrs3* Δ*mrs4* as the starting point. A number of synthetic lethal mutants (*tsa1, rad50, rad55,* and *dre2)* were non-viable when combined with Δ*mrs3* Δ*mrs4* but all were rescued by Rim2 overexpression (16). These genetic data suggested that Rim2 could be an iron transporter with functions overlapping those of Mrs3 and Mrs4. Finally, Gal-Rim2 repressed combined with Δ*mrs3* Δ*mrs4* yielded a more severe phenotype characterized by slower iron-dependent growth and more severe mitochondrial iron deficiency than the Δ*mrs3* Δ*mrs4* alone (13).

Author Manuscript Author Manuscript Author Manuscript Author Manuscript

Rim2 has been shown to transport iron more directly by organelle assays with isolated mitochondria. In mitochondria expressing Rim2, iron could be tracked from outside to inside using a porphyrin precursor and intramitochondrial heme synthesis as a surrogate for the transport activity. The transport activity required Rim2 expression and low (2–5 μM) concentrations of ferrous iron (13). An alternate assay involved mitochondrial membrane vesicles. These were loaded with Phen Green, a dye that can be quenched by iron binding, and the signal was monitored as it declined in a Rim2 and ferrous iron dependent manner (17).

Surprisingly, independent studies performed with bacterial expressed and purified Rim2 protein, reconstituted into vesicles, showed that Rim2 is a pyrimidine transporter (18). Transport activity was observed for pyrimidine (deoxy)nucleoside tri- and di-phosphates and to a lesser extent for pyrimidine (deoxy)nucleoside mono-phosphates. The transport was shown to operate by a counter exchange mechanism and exhibited saturation with a Km of 207 μM for TTP and a somewhat higher number for other nucleotides UTP and CTP (18). Pyrimidine nucleotides are needed in mitochondria for incorporation into DNA, mRNA, tRNA, rRNA and RNA primers, thereby being critical for replication, transcription, and translation. Since the nucleotide biosynthetic pathways reside outside mitochondria, Rim2-mediated transport in the physiologic setting is required to bring pyrimidine triphosphates into the mitochondrial matrix in exchange for export of pyrimidine monophosphates generated by mitochondrial metabolic processes. The transport of pyrimidine nucleotides was found to be sensitive to assay conditions with an optimum at 30–50 mM of NaCl and pH of 7 (18).

We wondered how a single mitochondrial carrier protein, Rim2, was capable of performing both functions i.e. the uptake and transport of ferrous iron into mitochondria and the uptake and transport of pyrimidine nucleotides into (and out of) mitochondria. The affinities for the two substrates appear to be very different, with the iron transport affinities lying in the low micromolar range and the pyrimidine transport affinities lying in the high micromolar range (18). The substrates are vastly different in size and shape, with TTP being about 3.3 angstroms in length and the ionic radius of iron being about 0.8 angstrom. The mechanisms of transport also appear to be different, with pyrimidine transport operating by an obligate exchange mechanism, whereas iron is taken up unidirectionally into mitochondria.

Rim2 has not been crystallized and the only structural information comes from extrapolation of the single available structure of the mitochondrial carrier family, that of the *Bos taurus* ADP/ATP carrier (19). Mitochondrial carrier proteins (MCP) contain triplications of linear sequences each of about 100 amino acids, containing 2 transmembrane (TM) domains and a flexible loop, thus giving the proteins a three-fold axis of symmetry. In the only known structure, a central core was visualized in the ADP/ATP carrier with carboxyatractyloside bound in the substrate-binding site of about 8 angstroms in diameter, and open to the intermembrane space (IMS) in the crystal structure (19). The mechanism of transport is thought to be a single binding center gated pore mechanism, according to which the substrate binds from the IMS side, leading to disruption of charge bridges between some of the helices (mediated by the sequence motif PX[DE]XX[RK]). A conformational change ensues and the substrate is released on the matrix side, while salt bridges reform on the IMS

Author Manuscript Author Manuscript Author Manuscript Author Manuscript

side. In many cases such as for Rim2 pyrimidine transport, there is an exchange such that substrate binding on the IMS side is followed by release of countersubstrate on the matrix side, followed by binding of a new substrate on the matrix side and flipping to the IMS side (20). For iron transport, however, it is unclear how Rim2-dependent transport might work, as the substrate is too small to fill the much larger substrate-binding pocket. Here we present the results of mutagenesis of Rim2 in which two critical exposed residues in the predicted substrate-binding pocket were mutated. The effects were dramatically different on the two transport activities. In one case, (E248A), the iron transport properties were disrupted and there was loss of proton coupled TTP/TMP exchange, whereas pyrimidine uptake was largely unaffected. For the other allele, (K299A), it was pyrimidine transport that was primarily affected, leaving iron transport largely intact.

2. Materials and Methods

2.1. Yeast strains and culture conditions.

The parental strain for this work was YS102–46 (*ura3-52 lys2-801 ade2-101 trp1-*Δ*63 his3-*Δ*200 leu2-*Δ*1 HIS3-GAL-RIM2::Rim2* Δ*mrs3::URA3* Δ*mrs4::KanMX)* which has a YPH499 background. *RIM2* expression was induced, where needed, by the addition of 0.5 % galactose to standard defined media with 2 % raffinose. This strain was transformed with YEp351 high copy-number plasmids carrying wild type Rim2, Rim2 (E248A), Rim2 (K299A), or vector alone. Transformants were selected and grown on defined medium lacking leucine (CSM-leu). Strain J116 *(MATa ura3 his3 leu2 ade2 ade3 cyh2* Δ*mrs3::TRP1* Δ*mrs4::HIS3 tsa1–116* [pTSV31A-*URA3*-2micron-*ADE3-MRS4*]), used in the sectoring assay, has been previously described (16). For preparation of mitochondria, strains bearing the YEp351 based constructs were streaked from −80°C glycerol stocks to CSM-leu, 2 % raffinose, 0.5 % galactose agar. Colonies were inoculated into CSM-leu 2 % raffinose and grown for a total of 40 h, with two successive sub-inoculations, to an OD_{600} of about 2. Cells were harvested by centrifugation and mitochondria were isolated as described (3).

2.2. Measurement of mitochondrial iron uptake and incorporation into heme.

Intact mitochondria equivalent to 200 μg of proteins were energized by incubating in HS buffer (50 mM Hepes/KOH pH 7.5, 0.6 M sorbitol containing 5 mM NADH. Protoporphyrinogen (10 μM final) (9) was added, and mitochondria were incubated at room temperature for 3 min, allowing *de novo* synthesis of porphyrins. ^{55}Fe (5 μM final) was added as ferrous ascorbate, and the incubation was allowed to continue for 5 min. Heme was extracted with acidic methylethylketone (21), and ^{55}Fe incorporated into heme was quantified by liquid scintillation counting.

2.3. Fe-S cluster synthesis assays.

The kinetics of Fe-S cluster synthesis under different conditions was ascertained in isolated intact mitochondria by incubation in the presence of ^{35}S-cysteine, nucleotides (2 mM NADH, 4 mM ATP, 1 mM GTP), with added iron (10 μM ferrous ascorbate). The radiolabeled [Fe-^{35}S] cluster inserted into endogenous aconitase was visualized by native gel electrophoresis and autoradiography (3).

Author Manuscript Author Manuscript Author Manuscript Author Manuscript

2.4. TTP transport assays.

TTP and dTTP uptake and export were tested in isolated mitochondria in the same buffers and time frames used for measuring heme synthesis. Intact mitochondria in HS buffer containing 50 mM NaCl were incubated with 260 nM tritiated TTP (thymidine 5' triphosphate [methyl ^{3}H] tetra sodium salt, MP Biomedical) or 48 nM dTTP (deoxy-thymidine 5' triphosphate [methyl ^{3}H] tetra sodium salt, MP Biomedical) for 5 min at room temperature. Mitochondria were recovered by centrifugation, and mitochondria-associated radioactivity was determined by scintillation counting. For export, mitochondria were incubated with radioactive TTP for 5 min at room temperature, and mitochondria were recovered. Fresh buffer was added with or without counterions, and an additional incubation was performed for 10 min at room temperature. After centrifugation, supernatant and pellet fractions were separated, and radioactivity was measured for each fraction (13, 18).

2.5. In-gel aconitase activity assay.

Mitochondria were lysed in buffer consisting of 50 mM Tris/HCl pH 8, 50 mM NaCl, 1% Triton X-100, 10% v/v glycerol, 2 mM Na-citrate and 15 U catalase. Samples were loaded on a native acrylamide gel containing 132 mM Tris base, 132 mM boric acid, 3.6 mM sodium citrate. The signal was developed in the gel by incubating in buffer containing 100 mM Tris/HCl, pH 8, 1 mM NADP, 2.5 mM *cis*-aconitic acid, 5 mM $MgCl_2$, 1.5 mM methylthiazolyldiphenyl-tetrazolium bromide (MTT), 0.3 mM phenazine methosulfate, and 5 U/ml isocitrate dehydrogenase (22, 23).

2.6. Miscellaneous procedures.

Protoporphyrinogen was prepared from protoporphyrin IX by reduction with sodium amalgam (24). Western blots were visualized with infra-red labeled secondary antibodies detected by a LiCor Odyssey instrument.

3. Results

3.1. Substitution of amino acids proposed to be involved in Rim2 substrate binding

Rim2 is a member of the mitochondrial carrier family (MCF) of proteins. This family of proteins is responsible for the translocation of nucleotides, amino acids, keto acids, vitamins, and inorganic ions across the mitochondrial inner membrane. Overall the transporter has a tripartite structure consisting of tandemly repeated domains of about 100 amino acids each (19). These domains contain two hydrophilic membrane segments connected by a hydrophilic loop. The ensemble folds into large membrane interacting entity in mitochondria forming a barrel with a central cavity through which substrates can pass. The central pocket contains amino acids having asymmetric features i.e. they do not align well with the other triplicated segments. Kunji and coworkers (20) reasoned that the residues that depart from symmetry might be involved in substrate binding, consistent with the generally asymmetric nature of binding substrates, the latter of which include amino acids, nucleotides, and carboxylic acids among other molecules. Rim2 was self-aligned by selecting the triplicated amino acid segments using the ClustalW program. Triplets (3 amino acids at a particular position in the alignment) were ascertained as in the analysis by Kunji and coworkers (20),

Author Manuscript Author Manuscript Author Manuscript Author Manuscript

and those triplets with exposure to the predicted substrate-binding pocket based on alignment with the ADP/ATP carrier structure were identified (Fig. 1A, teal).

Two charged residues E248 in helix 4 and K299 in helix 5 (Fig. 1B, red and blue circles, respectively), were identified as important because of their asymmetry, probable substrate-binding pocket exposure, and limited conservation in the nucleotide binding subclass of carrier proteins, suggesting an interaction with a specific substrate. They were individually mutated to alanine, and the transport properties of the mutants were studied in more detail. In particular, we were interested in the relative effects of the mutations on Rim2-mediated iron transport versus pyrimidine transport.

3.2. Genetic approach to evaluate Rim2 mutations for effects on iron transport independent of effects on pyrimidine transport

We devised a genetic approach to evaluate Rim2 mutations for *in vivo* effects on iron transport independent of effects on pyrimidine transport. The idea was that Rim2 holds tight synthetic lethal relationships with genes implicated in iron metabolism. Specifically Mrs3 and Mrs4, mitochondrial carrier proteins implicated in mitochondria iron import, are synthetically lethal with loss of function of Tsa1, a peroxiredoxin. The phenotype is both air and iron dependent (data not shown and (15, 16)). If we introduce Rim2 into this strain, the synthetic lethality is alleviated. To test if the mutant Rim2 proteins would also alleviate the lethality, a colony sectoring approach was used. The parent strain, J116 Δ*mrs3* Δ*mrs4 tsal-116* Δ*ade3* Δ*ade2,* was covered by the plasmid carrying *MRS4-ADE3*. This strain was unable to lose the covering plasmid, producing only red colonies (Fig. 2A, all red colonies) as a consequence of retaining the *ADE3* gene on the plasmid and accumulating adenine precursor pigment. In the presence of Rim2 introduced on a high copy-number plasmid, the *MRS4-ADE3* plasmid could be lost, and white or red-white sectoring colonies appeared (Fig. 2B, red, white and sectored colonies). These effects are very likely due to iron transport activity of Rim2, because Mrs3 or Mrs4 have not been implicated in other functions and neither one exhibits pyrimidine transport ability (our unpublished data). Control strains harboring *MRS3* (Fig. 2C) or *MRS4* (Fig. 2F) exhibited the predicted phenotypes (Fig. 2C, and 2F, red, white and sectored colonies). In two separate experiments, the *rim2* mutated alleles and controls were inserted into J116. In the first experiment uracil was present in the incubation prior to plating allowing more time for plasmid loss, whereas in the second experiment uracil was absent during the preincubation. The data for the two experiments, depicted in Table 1, are very similar. The E248A mutant did not allow any plasmid loss (Fig. 2D, red colonies only, 0% white or sectored in Expt. 1 and Expt. 2). On the other hand, the K299A mutant allowed significant plasmid loss (Fig. 2E, red and white colonies, 28% white or sectored in Expt. 1 and 14% in Expt 2.). Thus, the Rim2 (K299A) was still functional for iron transport, and was able to bypass the lack of Mrs3/4. By contrast, the Rim2 (E248A) had lost iron transport capability and could no longer bypass the lack of Mrs3/4. The number of white or sectored colonies in Rim2 (K299A), equal to 28% or 14%, however, appears to be somewhat less than in Rim2 (WT), equal to 80% or 36% (Table 1). The explanation for this is likely to be that there is a small effect of the K299A mutation on *in vivo* mitochondrial iron uptake, although very minor compared with the abrogating effect on *in vivo* pyrimidine transport.

Author Manuscript Author Manuscript Author Manuscript Author Manuscript

3.3. Splitting the functions of Rim2

The prediction from these genetic results is that Rim2 would function as an iron transporter for mitochondria and that the E248A mutation would abrogate this activity. This hypothesis was more directly tested. The high-copy plasmids carrying wild-type Rim2 (WT), Rim2 (E248A), Rim2 (K299A) or vector control (Vec) were introduced into a Gal-Rim2 Δ*mrs3/* Δ*mrs4* strain, and mitochondria were isolated from cells grown under repressing conditions in which Rim2 was not expressed from the chromosome but only from the plasmid. Iron uptake to mitochondria was evaluated using a porphyrin-based assay in which protoporphyrinogen (PPO) was added to the isolated and intact mitochondria, allowing a burst of protoporphyrin IX (PPIX) formation within mitochondria. ^{55}Fe was then added to the intact mitochondria as 10 μM ferrous ascorbate. After a 5 min incubation, newly formed radiolabeled heme was extracted using methylethylketone and quantified by scintillation counting. The assay is completely dependent on porphyrin IX synthesis and ferrochelatase (Hem15) activity inside the mitochondria. It reflects rate limiting iron transport from the mitochondrial intermembrane space to the matrix and is not beset by problems arising from nonspecific binding of iron to mitochondrial membranes (25). In highly reproducible results, we found that vector alone did not support uptake whereas wild-type Rim2 conferred a 5-fold increase (Fig. 3A).

The Rim2 (K299A) mutant was similar to the wild-type Rim2, indicating no loss of function for iron transport. By contrast, the E248A mutant was severely impaired, with iron uptake only slightly above the vector control, thus indicating severely compromised iron uptake activity. The flip side of the coin was examined, measuring the activity for the other transport substrate for Rim2 i.e. pyrimidine nucleotides. We used tritiated TTP because this has been shown to be the optimal substrate (18). ^{3}H-TTP uptake into isolated mitochondria repressed for Rim2 expression and carrying vector alone revealed a low basal activity (Fig. 3B). This baseline activity could be due to some slight leaky Rim2 expression or utilization of other transporters such as Ggc1, the GTP/GDP exchanger, which may also have some activity for TTP (18). Wild-type Rim2 dependent ^{3}H-TTP uptake activity was about 4-fold above the vector alone values, but as regards the mutants an inverse pattern was observed compared to the iron uptake. E248A was highly active, whereas K299A was entirely inactive, showing basal levels of uptake or even less. In summary, Rim2- mediated iron transport was dependent on E248, but not on K299, whereas TTP uptake was dependent on K299, but not on E248; the two transport activities were thus separated by individual mutations of these amino acids.

3.4. Rim2-dependent metal transport

When Rim2 up (galactose present during cell growth) was compared to Rim2 down (galactose absent during cell growth) in the Δ*mrs3* Δ*mrs4* background, there is generally a window of a 4-fold increment of iron into heme, reflecting Rim2-dependent iron transport. If iron and TTP are both Rim2 substrates and they share a common binding site, we reasoned there should be competition for uptake. Conversely, if the transported substrate is TTP-Fe perhaps with iron liganded to the phosphates of the nucleotide, then transport should be enhanced by forming the complex (17). In fact, we saw neither of these results. Following addition of unlabeled TTP in 1:1 or 1:20 molar excess over the iron radionuclide in the

Author Manuscript Author Manuscript Author Manuscript Author Manuscript

mitochondrial uptake reaction, there was no discernable effect on Rim2-dependent iron incorporation into heme. The binding sites may be different and/or distinct transport mechanisms may mediate transport of the distinct substrates, but there was no competition or enhancement of the iron uptake (Fig. 4A).

We then performed a series of experiments measuring Rim2-dependent mitochondrial iron uptake and incorporation into heme in the presence of a variety of metals (Ca, Mg, Be, Zn, Cu Cd, Co, Ni, Mn) (Fig. 4B). Some had no inhibitory or competitive activity at all. These included large and physiologically abundant group 2 cations such as calcium and magnesium. In addition, beryllium, a group 2 metal but with a radius smaller than iron, showed no competition for uptake. On the other hand, zinc, copper, cadmium, and cobalt, interfered with iron uptake and heme synthesis even at molar equivalence with iron. A different pattern was exhibited by Ni and Mn which were less severely inhibitory. A caveat to the inhibitory effects is that some of these metals may have an inhibitory effect on ferrochelatase. Ferrochelatase activity is a necessary component for our iron uptake assay. In the following order Cu > Zn > Co > Ni are all substrates for ferrochelatase (essentially compete with Fe). Mn and Cd are considered inhibitors of ferrochelatase, but are in fact incorporated into the porphyrin ring, but the metallated product is not released from the enzyme (26, 27).

3.5. Rim2-dependent pyrimidine exchange

Since Rim2 is an obligate exchanger for pyrimidine nucleotides, we tested the effects of different countersubstrates on Rim2-dependent export of TTP from mitochondria. This required a two-step assay in which Rim2 expressing mitochondria were preloaded with ^{3}H-dTTP. Then after removal of excess radioactivity, the counter substrate (TTP or TMP) was added for a brief period (5 min), centrifuged, and export was assessed by separating mitochondrial pellet from supernatant. Pyrimidine nucleotide uptake and exchange were tested for isolated mitochondria expressing vector alone (Vec), Rim2 WT, E248A mutant, or K299A mutant. The experiment was performed several times. In Fig. 5A, the data are shown as the percentage of the total ^{3}H-TTP initially loaded into mitochondria with the nucleotide remaining in mitochondria in dark gray and the ^{3}H-TTP in the supernatant in light gray. The data are averages from 3 replicates. In Fig. 5B, a single experiment is depicted, but in this case the data are shown as radioactivity (cpm) of ^{3}H-TTP either retained in mitochondria after exchange, dark gray, or released into the supernatant, light gray.

For the WT Rim2, export was efficient and occurred in response to TTP or TMP as counter ions, yielding a small residual ^{3}H-TTP pool (Fig. 5A and 5B). The vector (Vec) alone transformant (no Rim2 expressed) had a low level of exchange with or without counterions present (Fig. 5A and 5B). Note that Rim2 independent pyrimidine nucleotide uptake, albeit decreased, was sufficient that exchange could be assessed. For Rim2 (K299A), nucleotide uptake was decreased (Fig. 3B), but sufficient uptake still took place that export could be assessed (Fig. 5A and5B). There was little or no export regardless of the countersubstrate i.e. none (–), TTP or TMP. Also, addition of ATP, GTP or other nucleotides made no difference since there was little or no export (data not shown). An interesting result was obtained with the E248A mutant. In this case, ^{3}H-TTP export was nucleotide specific, occurring efficiently

Author Manuscript Author Manuscript Author Manuscript Author Manuscript

in response to the TTP counter substrate (40% mitochondrial ^{3}H-TTP remaining) but not with TMP as a counter substrate (70% mitochondrial ^{3}H-TTP remaining) (Fig. 5A). A possible explanation for this is that the E248 is involved in proton coupled transport and that the TTP-TMP exchange requires proton compensation (20). The E248 amino acid resides on TM4 in the substrate-binding pocket and lies in close proximity to the K299 on TM6, based on the homologous ADP/ATP carrier structure. According to a proposed transport mechanism (28), during the nucleotide transport process, a proton binds to E248 neutralizing the negative charge (pKa may be in the range of 4 for this membrane buried residue), thereby permitting binding of the negatively charged TTP phosphate to the positively charged K299. The transporter then shifts from an IMS-facing to a matrix-facing configuration as salt bridges are broken and reformed. The proton and nucleotide are then released to the matrix side. Such proton coupling is necessary for TTP- TMP heteroexchange and not for TTP-TTP homoexchange because of the charge imbalance (^{3}H-TTP out for TMP in might require 2 protons as compensation to equalize the charge). How this structural arrangement influences Rim2- mediated iron uptake is less clear, but iron might bind directly to E248 or might bind via a proton coupled mechanism as used by DMT1 (see Discussion).

3.6. Rim2-dependent TTP transport is salt dependent

The carriers have a tripartite structure with three homologous segments of about 100 amino acids, each consisting of 2 TM domains and a conserved signature motif PX[D/E]XX[K/R]X(K/R)x20– 30[D/E]GXXXX[W/Y/F][K/R]G, responsible for forming a network of cytoplasmic and matrix charge bridges. The single substrate-binding site gated pore mechanism of the carriers involves the breaking of the charge network on the matrix side and reforming bridges on the cytoplasmic side. To optimize Rim2-dependent pyrimidine transport, the basic buffer 50 mM Hepes/KOH, pH 7.4 was modified to vary the salt concentration from 0–100 mM NaCl. Rim2- dependent ^{3}H-TTP uptake was found to be almost entirely salt dependent (Fig. 6A). The mitochondrial uptake in the absence of salt was 249 cpm, equivalent to the uptake in the absence of Rim2 expression. The activity was maximum between 25–50 mM NaCl and decreased somewhat at higher concentrations of salt. By contrast, Rim2-dependent heme synthesis reflecting iron uptake into mitochondria was 72% of maximum even with no salt, and the curve was flat between 25 and 75 mM suggesting independence of the salt concentration. The results suggest fundamental differences in the transport mechanisms for pyrimidines and iron.

3.7. Effects of metal competition on Rim2-dependent TTP uptake

If the pyrimidine nucleotides and iron share a common binding site on Rim2, we might see inhibition of ^{3}H-TTP uptake in the presence of excess added iron. If the pyrimidines and iron are obligately co-transported, we might see enhancement of TTP uptake in the presence of added iron. Instead, the results showed no effect on ^{3}H-TTP uptake of the addition of ferric ammonium sulfate or ferrous sulfate during the assay, even when present in a large molar excess of 1000X (Fig. 6B. top panel).

Author Manuscript Author Manuscript Author Manuscript Author Manuscript

3.8. In vivo mitochondrial phenotypes of the rim2 mutants

The set of mitochondria expressing the different Rim2 alleles was further investigated, seeking more in-depth characterization of their phenotypes. First, immunoblotting was performed (Fig. 7A). Rim2 expression was very low in the vector alone (Vec) but still detectable consistent with leaky expression from the repressed chromosomal *GAL1* promoter, even though the cells were grown for 14 h in raffinose in the absence of galactose. For the Rim2 expressing cells, levels were high but comparable to each other in WT, E248A and K299A mitochondria, reflecting strong and roughly equivalent expression from the 2 micron plasmids. Interestingly, effects of iron deprivation could be discerned in the Vec and E248A mitochondria. Aconitase is an abundant mitochondrial protein and the biosynthesis of its [4Fe- 4S] cluster cofactor requires mitochondrial iron. Aconitase activity was higher in WT and K299A mitochondria than in Vec and E248A mitochondria, reflecting iron starvation in the latter set (Fig. 7B). Aconitase protein was only modestly affected, with slightly lower levels in Vec and E248A, indicating that during the time course of the experiment, the apoprotein was slightly destabilized (Fig. 7A). Lipoic acid is a cofactor synthesized exclusively in mitochondria and dependent on Lip5, a radical SAM enzyme with two distinct [4Fe-4S] clusters and therefore susceptible to mitochondrial iron limiting conditions. The lipoic acid content was evaluated by immunoblotting with an antibody for the lipoic acid cofactor, and signals for lipoic acid containing proteins Lat1, the dihyrolipoamide acetyl transferase E2 component of the pyruvate dehydrogenase complex, and Kgd2, the dihyrolipoamide transsuccinylase E2 component of the alpha ketoglutarate dehydrogenase, were evaluated. There were marked decreases of both in the E248A compared to the K299A mutant. The E248A mutant resembled vector alone in this case indicating lipoic acid deficiency in these mitochondria, likely a result of iron starvation. Finally, cytochrome *c* was evaluated by immunoblotting of mitochondria. Cytochrome *c* is a heme protein residing in the intermembrane space, and its abundance reflects mitochondrial heme synthesis, because transcription is heme dependent, and the apoprotein is unstable and rapidly turned over. The relative decrease observed in the Vec and E248A versus WT and K299A are probably the result of *in vivo* iron deficiency. Nfs1 and porin protein levels and the overall Ponceau S red protein stain were unaffected by the mutations as expected and served as controls (Fig. 7A). Finally, a kinetic Fe-S cluster loading experiment was performed (Fig. 7C). Isolated and intact mitochondria were supplemented with ATP, GTP, and NADH, and incubated with ^{35}S-cysteine to allow continuous synthesis of new Fe-^{35}S clusters and insertion into endogenous apo-aconitase. The WT loaded efficiently, Vec alone had negligible activity. The K299A evidenced more loading activity than the E248A although residual activity was still present indicating a partial loss of function in this mutant.

In summary, various *in vivo* phenotypes support the conclusion that the mitochondria expressing the E248A Rim2 allele were impaired for iron-related functions whereas the K299A mitochondria were not. We were surprised at the significant amount of residual aconitase enzyme activity and loading activity in the E248A mutant compared with empty vector, especially given that the same mutant exhibited negligible mitochondrial iron uptake into heme. It may be worth noting that the iron transport measurements reflect iron delivery into the mitochondrial matrix for heme synthesis. On the other hand, the aconitase measurements (activity and loading) reflect iron delivery for Fe-S cluster synthesis. It is

Author Manuscript Author Manuscript Author Manuscript Author Manuscript

possible that the Rim2 transporter might have some specificity in delivering iron for heme in preference to Fe-S cluster synthesis. Alternatively, heme synthesis and Fe-S cluster synthesis in mitochondria might have different thresholds for available iron (Fe-S synthesis having a lower more accessible threshold).

4. Discussion

The mitochondrial carrier proteins constitute a large protein family present in the inner membrane of mitochondria (29, 30). Homologs are not found in bacteria, so the evolutionary origins are mysterious. These proteins move various kinds of substrates across the mitochondrial inner membrane in both directions, sometimes as exchangers and sometimes as uniporters. Occasionally the transport mechanism is proton coupled and can be driven by protons of the mitochondrial membrane potential (28). The substrates are varied but most famously include nucleotides such as ATP transported by the ADP/ATP exchanger, which mediates export of ATP synthesized by the ATP synthase in the mitochondrial matrix to rest of the cell (31). In many cases, the mitochondrial carriers link metabolic pathways that are compartmentalized between mitochondria and cytoplasm, with some steps taking place inside and some steps taking place outside (see for example the citric acid cycle, oxidative phosphorylation, amino acid and fatty acid metabolism) (29, 30).

Here we have focused on the Rim2 mitochondrial carrier protein. It has been well established that Rim2 transports pyrimidine (deoxy)nucleoside tri- and di-phosphates and to a lesser extent mono-phosphates (18). Biosynthesis of these nucleotides takes place outside mitochondria in the cytoplasm, and critical uses for them (replication, transcription, and translation) take place in mitochondria. The physiologic purpose of the transporter seems to be to bring these nucleotide triphosphates into the mitochondria in exchange for monophosphate forms generated in the course of mitochondrial metabolism. The critical nature of this function is evidenced by the sick or non-viable condition of the deletion mutants. The assays that established the role of Rim2 in pyrimidine transport include intact organelle assays showing uptake and exchange of pyrimidines (13, 17, 18) and vesicle assays in which purified protein was reconstituted into liposomes, which recapitulate homo exchange (e.g. TTP, TTP) and hetero exchange (e.g. TTP, TMP). The latter is apparently electroneutral but proton coupled (18).

We used the analysis performed by Kunji and coworkers for asymmetric triplets (20) to identify critical residues in the Rim2 binding site that might interact with the pyrimidine nucleotide substrate. Asymmetric residue K299 (of triplet 18, GG**K**) on TM region H5 was predicted to be exposed to the substrate-binding cavity (Fig. 1). It was speculated that that the positive charge of K299 promotes interaction with the negatively charged phosphates of the pyrimidine (deoxy)nucleotide substrates (20). The prediction is supported by our experiments, since the K299A mutation entirely abrogated pyrimidine uptake and pyrimidine exchange (Fig. 3B and Fig. 5). A second oppositely charged asymmetric residue E248 (of triplet 83, A**E**N) on TM region H4 was also predicted to be exposed to the substrate and was targeted by mutagenesis. In the Rim2 E248A mutant, homo exchange was minimally, if at all, affected but hetero exchange of TTP for TMP was blocked (Fig 5). It is likely that the asymmetric E248, predicted to have a low pKa in the membrane (28), is

Author Manuscript Author Manuscript Author Manuscript Author Manuscript

involved in proton coupling, allowing charge neutralization during the TTP/TMP exchange (Fig. 5).

The unique and most interesting feature of Rim2 is that it functions both as a (deoxy)pyrimidine nucleotide exchanger of the mitochondrial inner membrane and an iron importer. Rim2 involvement in mitochondrial iron uptake is supported by whole cell studies in which it either worsens (loss of function) or bypasses (overexpression) Δ*mrs3* Δ*mrs4* iron-dependent growth and mitochondrial iron protein phenotypes (13). Organelle studies also demonstrate Rim2-dependent iron transport into mitochondria for heme synthesis from added porphyrin precursors (Fig. 3A). Studies with submitochondrial particles (SMPs) vesicles derived from mitochondrial membranes expressing Rim2 have also shown iron transport (17). However, the reconstituted purified Rim2 protein has not been examined for iron transport thus far. The question arises of how Rim2 can transport both pyrimidine nucleotides and iron ions, given that they are vastly different in size (3.3 versus 0.8 angstroms), charge (−3 versus +2), and physiologic abundance (nucleotides are present in much greater quantities than micronutrients such as iron).

An attractive idea is that iron ion might bind to and “piggyback” on the nucleotide substrate during the transport process. It is known that the phosphates of NTPs may coordinate metal ions. There is a well-characterized mitochondrial transporter, Sal1, that is able to mediate ATP-Mg^{2+} transport in exchange for phosphate anion (32). Froschauer et al. (17) used SMPs from mitochondrial membranes expressing Rim2 to study iron uptake and found cotransport of Fe^{2+} and pyrimidine nucleotide triphosphates. However, these studies were not performed with purified reconstituted transporters, and the SMPs were probably inside out in their orientation (33), and so in these studies the transport direction could have been reversed from the physiologic one.

Our studies do not support cotransport of pyrimidines and iron as a mechanism of Rim2-dependent iron uptake into mitochondria. Various biochemical parameters of the iron versus pyrimidine nucleotide transport suggest that the two processes occur independently. The absolute dependence on salt for pyrimidine nucleotide transport (Fig. 6A), contrasts with the relative independence for iron uptake (Fig. 6A). In terms of competition, iron has no enhancing or inhibiting effect on Rim2-dependent pyrimidine transport (Fig. 6B). Conversely, pyrimidines nucleotides do not influence iron uptake (Fig. 4A). Finally, the mutant alleles of Rim2 had distinct effects on pyrimidine nucleotide transport and iron transport. The K299A blocked pyrimidine nucleotide transport entirely while having no effect on iron uptake. The E248A had little effect on pyrimidine uptake although hetero exchange of TTP and TMP was impaired. More importantly, the ferrous iron uptake was abrogated (Fig. 3). *In vivo* studies confirmed the E248A effects on iron dependent functions in mitochondria. Mutant mitochondria expressing Rim2 E248A in the Δ*mrs3* Δ*mrs4* context showed signs of iron deficiency clearly distinct from the Rim2 K299A mitochondria which showed no signs of iron deficiency. The E248A mitochondria demonstrated deficiencies of lipoic acid-containing proteins (dependent on Fe-S protein Lip5), and cytochrome *c* (dependent on heme synthesis), as well as aconitase activity deficiency. The kinetics of aconitase loading with newly made Fe-S clusters was slowed in the E248A versus the

Author Manuscript Author Manuscript Author Manuscript Author Manuscript

K299A mitochondria, although there clearly was residual activity compared with the no-Rim2 control mutants (Fig. 7C).

We are left with the question, if iron transport by Rim2 does not occur by cotransport with pyrimidines, then how does it occur? Mrs3 and Mrs4 can perform a similar function to Rim2 as they are physiologically redundant with Rim2, and they are able to transport iron into mitochondria. Critical asymmetric residues in the substrate-binding site of Mrs3 include two histidine residues, one on helix 1, H48, and one on helix 2, H105, which could be involved in direct metal interactions. Mutation of histidine 105 to adenine abrogates iron transport (our unpublished data and (34)). Interestingly, Rim2 also has an asymmetric histidine H354 in triplet 76 (Fig. 1A, NS**H**) exposed to the substrate- binding cavity, and this might directly bind iron during the transport process. Proton coupling is thought to occur during Mrs3 (20) and Rim2 (20) mediated transport. Perhaps as in the case of the H^+ coupled endosomal iron transporter DMT1 (35), a proton binds to the acidic residue E248 producing charge neutralization and a conformational change that then promotes ferrous binding to the exposed histidine 354 nearby in the substrate-binding pocket. The small size of the iron ion would not fill the substrate-binding cavity, and perhaps it is liganded to a larger molecule such as phosphate during transport. A shift of the transporter conformation from IMS to matrix orientation would then occur, coordinated with release of the iron-ligand and proton into the matrix. Although Rim2 is an obligate exchanger of pyrimidine nucleotides (18), it is unknown if there is a counter substrate exchanged for the imported iron. Clearly more work, both structural and biochemical, will be needed to fully determine the Rim2-mediated iron transport mechanism.

Another example of a mitochondrial carrier protein with two dissimilar substrates has been recently described. In this case, Pic2, already known as a mitochondrial phosphate transporter in yeast, was found to be involved in copper transport as well (36). Cytochrome oxidase and Sod1, mitochondrial copper proteins are apparently metallated from a matrix copper pool. The formation of the matrix copper pool requires transport of copper cation, probably copper I, across the mitochondrial inner membrane into the matrix, and Pic2 was recently shown to be a key mediator of this process (36). The human homolog of Pic2, SLC25A3, was also shown to be involved in both copper and phosphate transport (37). Perhaps copper I, like iron II, is taken up via direct binding within the transport substrate site, and perhaps proton coupling during the transport process and substrate binding occur via juxtaposed negatively and positively charged residues in the binding pocket (D124 and R175 in Pic 2 [20,24]). How exactly an anion (phosphate) and cation (copper) can be transported by the same mitochondrial carrier protein transporter remains unclear, but the conundrum is strongly reminiscent of the Rim2 transport activities for both an anion (nucleotide triphosphate) and cation (ferrous iron) (38).

Acknowledgements:

This work was supported by National Institutes of Health Grant R37DK053953 (to A.D) and by RO1 GM107542 (to D.P. and A.D.) We are grateful to Edmund Kunji for discussions on the mechanism of Rim2 transport.

Author Manuscript Author Manuscript Author Manuscript Author Manuscript

References

1. Crichton R The importance of iron for biological systems. Inorganic biochemistry of iron metabolism Chichester, West Sussex, PO19 1 EB, England: Ellis Horwood Limited; 1991.
2. Holmes-Hampton GP, Miao R, Garber Morales J, Guo Y, Munck E, Lindahl PA. A nonheme high-spin ferrous pool in mitochondria isolated from fermenting Saccharomyces cerevisiae. Biochemistry. 2010;49(19):4227–34. [PubMed: 20408527]
3. Amutha B, Gordon DM, Dancis A, Pain D. Chapter 14 Nucleotide-dependent iron-sulfur cluster biogenesis of endogenous and imported apoproteins in isolated intact mitochondria. Methods Enzymol. 2009;456:247–66. [PubMed: 19348893]
4. Medlock AE, Shiferaw MT, Marcero JR, Vashisht AA, Wohlschlegel JA, Phillips JD, Dailey HA. Identification of the Mitochondrial Heme Metabolism Complex. PLoS One. 2015;10(8):e0135896. [PubMed: 26287972]
5. Foury F, Roganti T. Deletion of the mitochondrial carrier genes MRS3 and MRS4 suppresses mitochondrial iron accumulation in a yeast frataxin-deficient strain. J Biol Chem. 2002;277(27): 24475–83. [PubMed: 12006577]
6. Froschauer EM, Schweyen RJ, Wiesenberger G. The yeast mitochondrial carrier proteins Mrs3p/Mrs4p mediate iron transport across the inner mitochondrial membrane. Biochim Biophys Acta. 2009;1788(5): 1044–50. [PubMed: 19285482]
7. Moore MJ, Wofford JD, Dancis A, Lindahl PA. Recovery of mrs3Deltamrs4Delta Saccharomyces cerevisiae Cells under Iron-Sufficient Conditions and the Role of Fe580. Biochemistry. 2018;57(5): 672–83. [PubMed: 29228768]
8. Muhlenhoff U, Stadler JA, Richhardt N, Seubert A, Eickhorst T, Schweyen RJ, Lill R, Wiesenberger G. A specific role of the yeast mitochondrial carriers MRS3/4p in mitochondrial iron acquisition under iron-limiting conditions. J Biol Chem. 2003;278(42):40612–20. [PubMed: 12902335]
9. Zhang Y, Lyver ER, Knight SA, Lesuisse E, Dancis A. Frataxin and mitochondrial carrier proteins, Mrs3p and Mrs4p, cooperate in providing iron for heme synthesis. J Biol Chem. 2005;280(20): 19794–807. [PubMed: 15767258]
10. Zhang Y, Lyver ER, Knight SA, Pain D, Lesuisse E, Dancis A. Mrs3p, Mrs4p, and frataxin provide iron for Fe-S cluster synthesis in mitochondria. J Biol Chem. 2006;281(32):22493–502. [PubMed: 16769722]
11. Paradkar PN, Zumbrennen KB, Paw BH, Ward DM, Kaplan J. Regulation of mitochondrial iron import through differential turnover of mitoferrin 1 and mitoferrin 2. Mol Cell Biol. 2009;29(4): 1007–16. [PubMed: 19075006]
12. Shaw GC, Cope JJ, Li L, Corson K, Hersey C, Ackermann GE, Gwynn B, Lambert AJ, Wingert RA, Traver D, Trede NS, Barut BA, Zhou Y, Minet E, Donovan A, Brownlie A, Balzan R, Weiss MJ, Peters LL, Kaplan J, Zon LI, Paw BH. Mitoferrin is essential for erythroid iron assimilation. Nature. 2006;440(7080):96–100. [PubMed: 16511496]
13. Yoon H, Zhang Y, Pain J, Lyver ER, Lesuisse E, Pain D, Dancis A. Rim2, a pyrimidine nucleotide exchanger, is needed for iron utilization in mitochondria. Biochem J. 2011;440(1): 137–46. [PubMed: 21777202]
14. Van Dyck E, Jank B, Ragnini A, Schweyen RJ, Duyckaerts C, Sluse F, Foury F. Overexpression of a novel member of the mitochondrial carrier family rescues defects in both DNA and RNA metabolism in yeast mitochondria. Mol Gen Genet. 1995;246(4):426–36. [PubMed: 7891656]
15. Lin H, Li L, Jia X, Ward DM, Kaplan J. Genetic and biochemical analysis of high iron toxicity in yeast: iron toxicity is due to the accumulation of cytosolic iron and occurs under both aerobic and anaerobic conditions. J Biol Chem. 2011;286(5):3851–62. [PubMed: 21115478]
16. Zhang Y, Lyver ER, Nakamaru-Ogiso E, Yoon H, Amutha B, Lee DW, Bi E, Ohnishi T, Daldal F, Pain D, Dancis A. Dre2, a conserved eukaryotic Fe/S cluster protein, functions in cytosolic Fe/S protein biogenesis. Mol Cell Biol. 2008;28(18):5569–82. [PubMed: 18625724]
17. Froschauer EM, Rietzschel N, Hassler MR, Binder M, Schweyen RJ, Lill R, Muhlenhoff U, Wiesenberger G. The mitochondrial carrier Rim2 co-imports pyrimidine nucleotides and iron. Biochem J. 2013;455(1):57–65. [PubMed: 23800229]

Author Manuscript Author Manuscript Author Manuscript Author Manuscript

18. Marobbio CM, Di Noia MA, Palmieri F. Identification of a mitochondrial transporter for pyrimidine nucleotides in Saccharomyces cerevisiae: bacterial expression, reconstitution and functional characterization. Biochem J. 2006;393(Pt 2):441–6. [PubMed: 16194150]
19. Pebay-Peyroula E, Dahout-Gonzalez C, Kahn R, Trezeguet V, Lauquin GJ, Brandolin G. Structure of mitochondrial ADP/ATP carrier in complex with carboxyatractyloside. Nature. 2003;426(6962): 39–44. [PubMed: 14603310]
20. Robinson AJ, Overy C, Kunji ER. The mechanism of transport by mitochondrial carriers based on analysis of symmetry. Proc Natl Acad Sci U S A. 2008;105(46):17766–71. [PubMed: 19001266]
21. Teale FW. Cleavage of the haem-protein link by acid methylethylketone. Biochim Biophys Acta. 1959;35:543. [PubMed: 13837237]
22. Amutha B, Gordon DM, Gu Y, Lyver ER, Dancis A, Pain D. GTP is required for iron-sulfur cluster biogenesis in mitochondria. J Biol Chem. 2008;283(3):1362–71. [PubMed: 18029354]
23. Tong WH, Rouault TA. Functions of mitochondrial ISCU and cytosolic ISCU in mammalian iron-sulfur cluster biogenesis and iron homeostasis. Cell Metab. 2006;3(3): 199–210. [PubMed: 16517407]
24. Abraham NG, Camadro JM, Hoffstein ST, Levere RD. Effects of iron deficiency and chronic iron overloading on mitochondrial heme biosynthetic enzymes in rat liver. Biochim Biophys Acta. 1986;870(2):339–49. [PubMed: 3955059]
25. Lange H, Kispal G, Lill R. Mechanism of iron transport to the site of heme synthesis inside yeast mitochondria. J Biol Chem. 1999;274(27):18989–96. [PubMed: 10383398]
26. Dailey HA. Metal inhibition of ferrochelatase. Ann N Y Acad Sci. 1987;514:81–6. [PubMed: 3442391]
27. Hunter GA, Sampson MP, Ferreira GC. Metal ion substrate inhibition of ferrochelatase. J Biol Chem. 2008;283(35):23685–91. [PubMed: 18593702]
28. Kunji ER, Robinson AJ. Coupling of proton and substrate translocation in the transport cycle of mitochondrial carriers. Curr Opin Struct Biol. 2010;20(4):440–7. [PubMed: 20598524]
29. Palmieri F, Pierri CL, De Grassi A, Nunes-Nesi A, Fernie AR. Evolution, structure and function of mitochondrial carriers: a review with new insights. Plant J. 2011;66(1): 161–81. [PubMed: 21443630]
30. Walker JE, Runswick MJ. The mitochondrial transport protein superfamily. J Bioenerg Biomembr. 1993;25(5):435–46. [PubMed: 8132484]
31. Duncan AL, Ruprecht JJ, Kunji ERS, Robinson AJ. Cardiolipin dynamics and binding to conserved residues in the mitochondrial ADP/ATP carrier. Biochim Biophys Acta. 2018;1860(5): 1035–45.
32. Traba J, Froschauer EM, Wiesenberger G, Satrustegui J, Del Arco A. Yeast mitochondria import ATP through the calcium-dependent ATP-Mg/Pi carrier Sal1p, and are ATP consumers during aerobic growth in glucose. Mol Microbiol. 2008;69(3):570–85. [PubMed: 18485069]
33. Chance B, Mela L. Energy-linked changes of hydrogen ion concentration in submitochondrial particles. J Biol Chem. 1967;242(5):830–44. [PubMed: 6020437]
34. Brazzolotto X, Pierrel F, Pelosi L. Three conserved histidine residues contribute to mitochondrial iron transport through mitoferrins. Biochem J. 2014;460(1):79–89. [PubMed: 24624902]
35. Pujol-Gimenez J, Hediger MA, Gyimesi G. A novel proton transfer mechanism in the SLC11 family of divalent metal ion transporters. Sci Rep. 2017;7(1):6194. [PubMed: 28754960]
36. Vest KE, Leary SC, Winge DR, Cobine PA. Copper import into the mitochondrial matrix in Saccharomyces cerevisiae is mediated by Pic2, a mitochondrial carrier family protein. J Biol Chem. 2013;288(33):23884–92. [PubMed: 23846699]
37. Boulet A, Vest KE, Maynard MK, Gammon MG, Russell AC, Mathews AT, Cole SE, Zhu X, Phillips CB, Kwong JQ, Dodani SC, Leary SC, Cobine PA. The mammalian phosphate carrier SLC25A3 is a mitochondrial copper transporter required for cytochrome c oxidase biogenesis. J Biol Chem. 2018;293(6):1887–96. [PubMed: 29237729]
38. Winge DR. Filling the mitochondrial copper pool. J Biol Chem. 2018;293(6):1897–8. [PubMed: 29462794]

Author Manuscript Author Manuscript Author Manuscript Author Manuscript

A

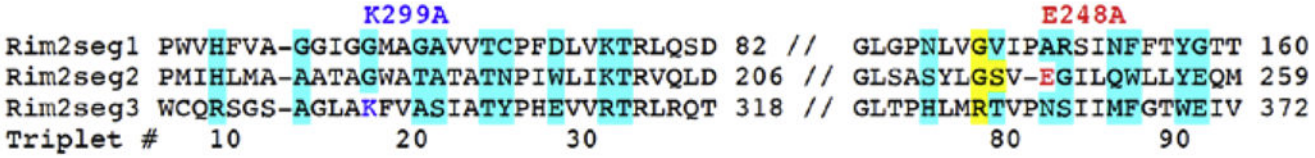

B

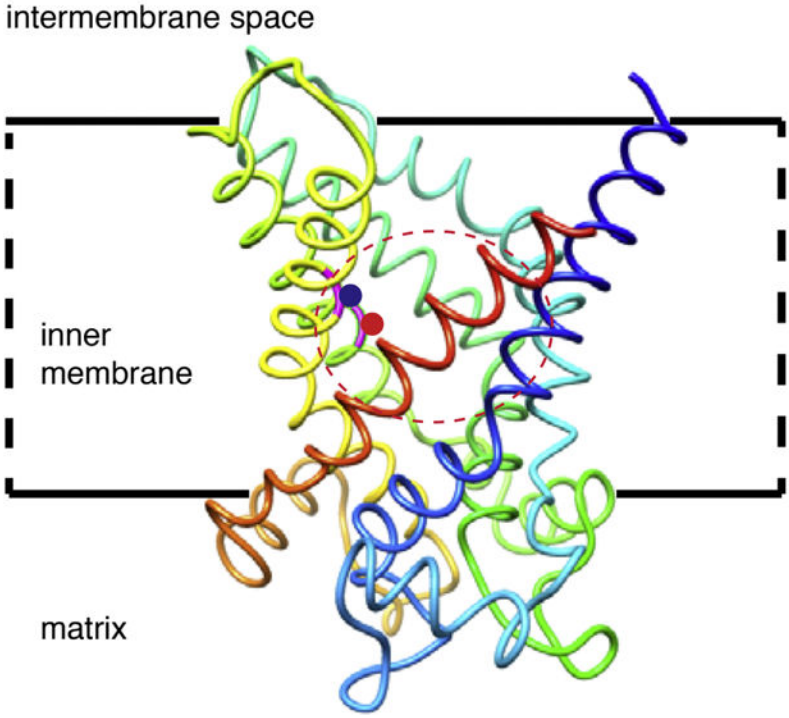

Fig. 1. Alignment of Rim2 homologous repeats and protein model based on structure of the ADP/ATP mitochondrial carrier.

(A) The three homologous repeats of Rim2 were aligned with ClustalW. Residues facing the protein cavity are highlighted in teal. Proposed pyrimidine contact points G145, G245, S246 and R357 are indicated in yellow. Potential proton coupler E248, and contact residue K299 are indicated in red and blue respectively. (B) The six helices of the mitochondria carrier are color coded from C-terminus; H1 blue, H2 cyan, H3 turquoise, H4 green, H5 yellow, and H6 red. Positions of residues E248 on H4 (red circle) and K299 on H5 (blue circle) are indicated. The position of the pyrimidine binding site within the cavity is circled.

Author Manuscript Author Manuscript Author Manuscript Author Manuscript

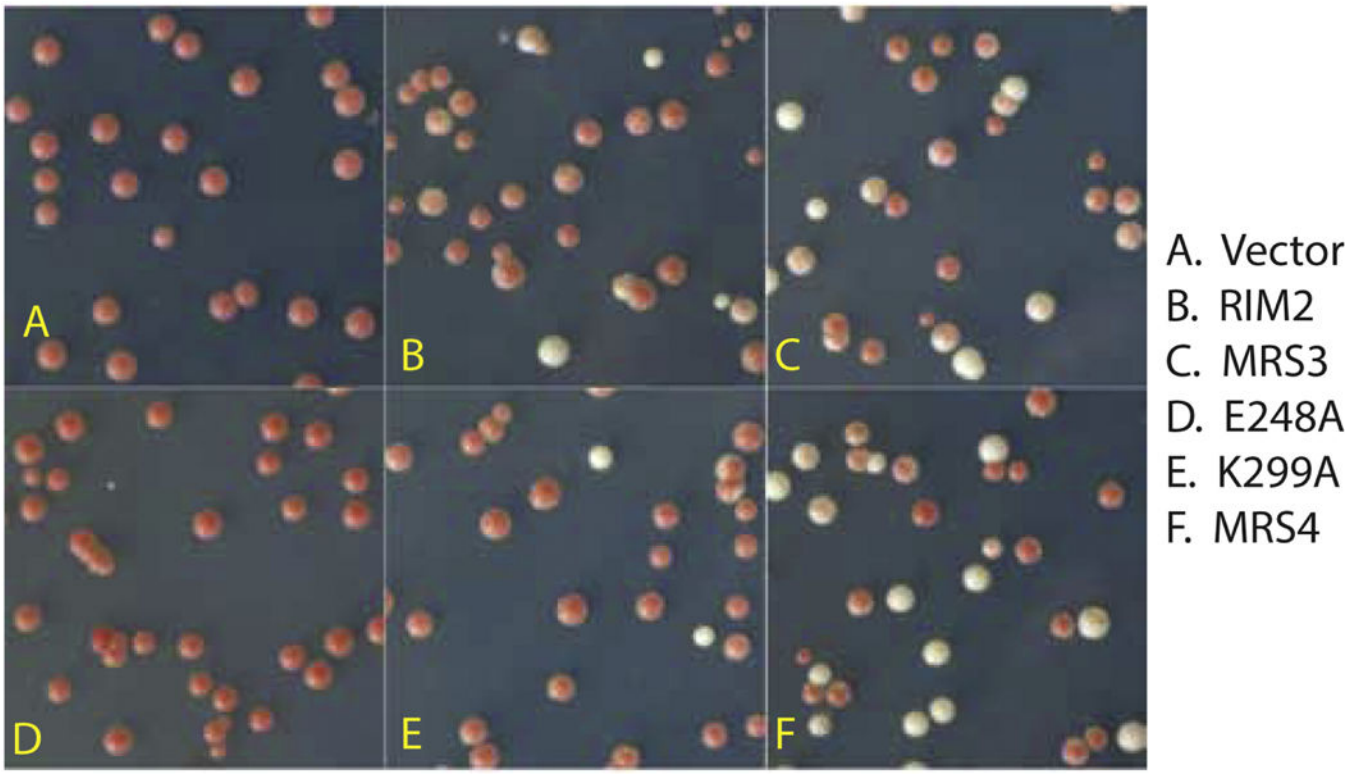

Fig. 2. Rim2 residue E248, but not K299, is essential for Rim2 complementation of cells lacking mitochondrial transporters Mrs3 and Mrs4.

Strain YS97–15 *(mrs3, mrs4, ade2, ade3* [pTSV31A-URA3-ADE3-MRS4]), was transformed with Yep351 vector with (A) vector alone, (B) Rim2, (C) Mrs3, (D) Rim2 (E248A), (E) Rim2 (K299A), and (F) Mrs4. Transformants from a CSM-ura-leu plate were grown 20 h in CSM-leu (no uracil selection) and plated onto CSM-leu plates. After 4 d at 30°C agar plates were photographed and red, white, and sectoring colonies were counted. Two experiments were performed. During the first experiment, uracil was present during the preincubation, whereas during the second experiment uracil was omitted. The numbers of red, sectoring, and white colonies in Experiment 1 and 2 are shown in Table 1.

Author Manuscript Author Manuscript Author Manuscript Author Manuscript

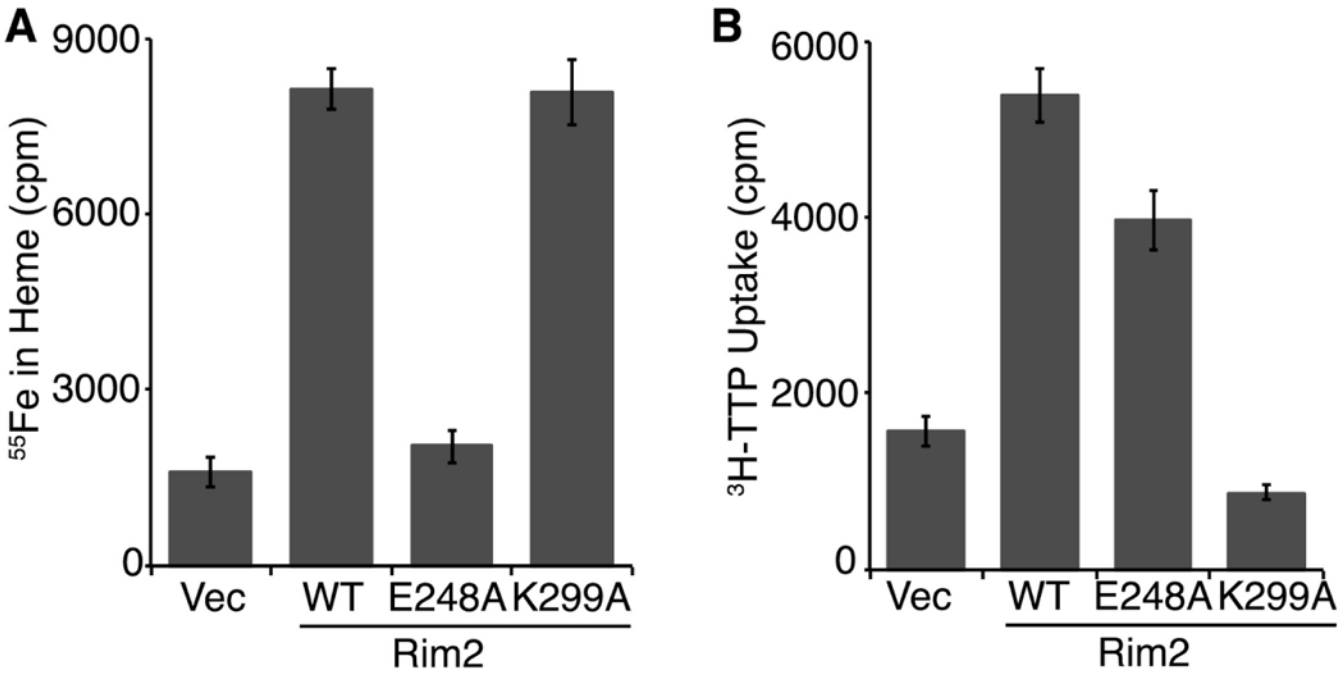

Fig. 3. Rim2 residue E428 is required for iron uptake, whereas residue K299 is required for pyrimidine uptake.

(A) Isolated mitochondria, from strain YS102–46 *(mrs3*Δ *mrs4*Δ *GAL-RIM2)* transformed with YEp351 (Vec), and YEp351 bearing: *RIM2* (WT), *rim2-E248A, rim2-K299A* and grown in the absence of galactose, were preloaded with PPO and incubated with ^{55}Fe-ascobate for 5 min at room temperature. Heme iron was extracted and the incorporated ^{55}Fe was quantified by liquid scintillation counting. Results show mean and SD (n=2) and represent one of three independent experiments. (B) Isolated mitochondria were incubated with ^{3}H-TTP for 5 min at room temperature, then centrifuged and washed in isotonic buffer to remove external ^{3}H-TTP. The washed mitochondria were lysed and ^{3}H- TTP was quantified by liquid scintillation counting. Results show mean and SD (n=2) and represent one of three independent experiments.

Author Manuscript
Author Manuscript
Author Manuscript
Author Manuscript

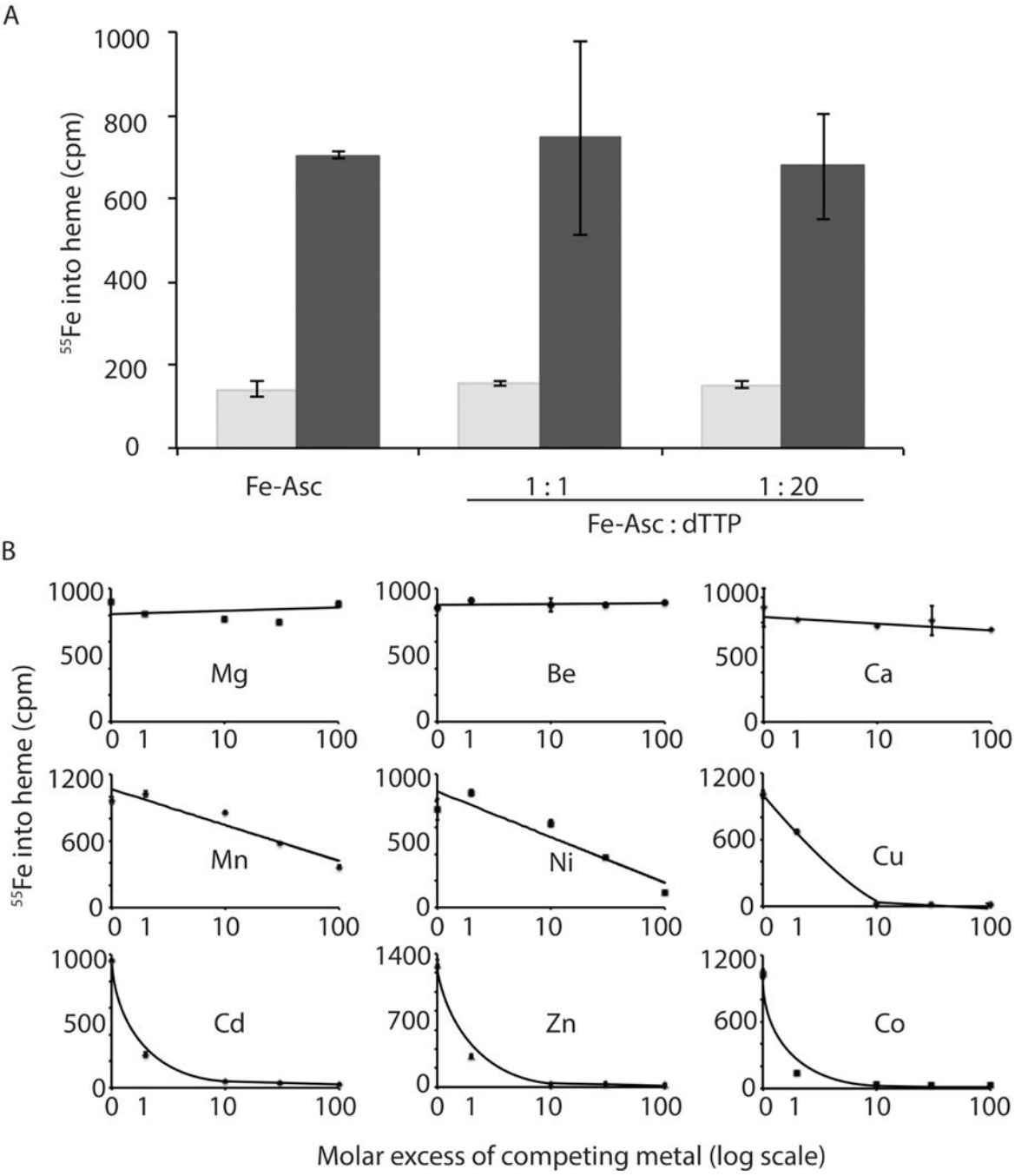

Fig. 4. Mitochondrial iron uptake is independent of dTTP and inhibited by d-block metals but not group 2 metals.

(A) Isolated mitochondria from strain YS102–46 grown in the presence (dark gray) or absence (light gray) of galactose, were incubated with ^{55}Fe-ascorbate (Fe-Asc), or ^{55}Fe-ascorbate that had been precombined in a 1:1 or a 1:20 molar ratio with dTTP. After 5 min incubation at room temperature heme was extracted and incorporated ^{55}Fe was quantified. Results show mean and SD (n=3) and represent one of two independent experiments. (B) Isolated mitochondria preloaded with PPO were incubated ^{55}Fe-Asc, or ^{55}Fe-Asc combined with indicated metal at molar ratios of 1:1, 1:10, 1:30, and 1:100. After 5 min incubation

heme was extracted and incorporated ^{55}Fe quantified by liquid scintillation counting. Each experiment was performed in duplicate and error bars (where visible) represent the range of the two values.

Author Manuscript Author Manuscript Author Manuscript Author Manuscript

Author Manuscript Author Manuscript Author Manuscript Author Manuscript

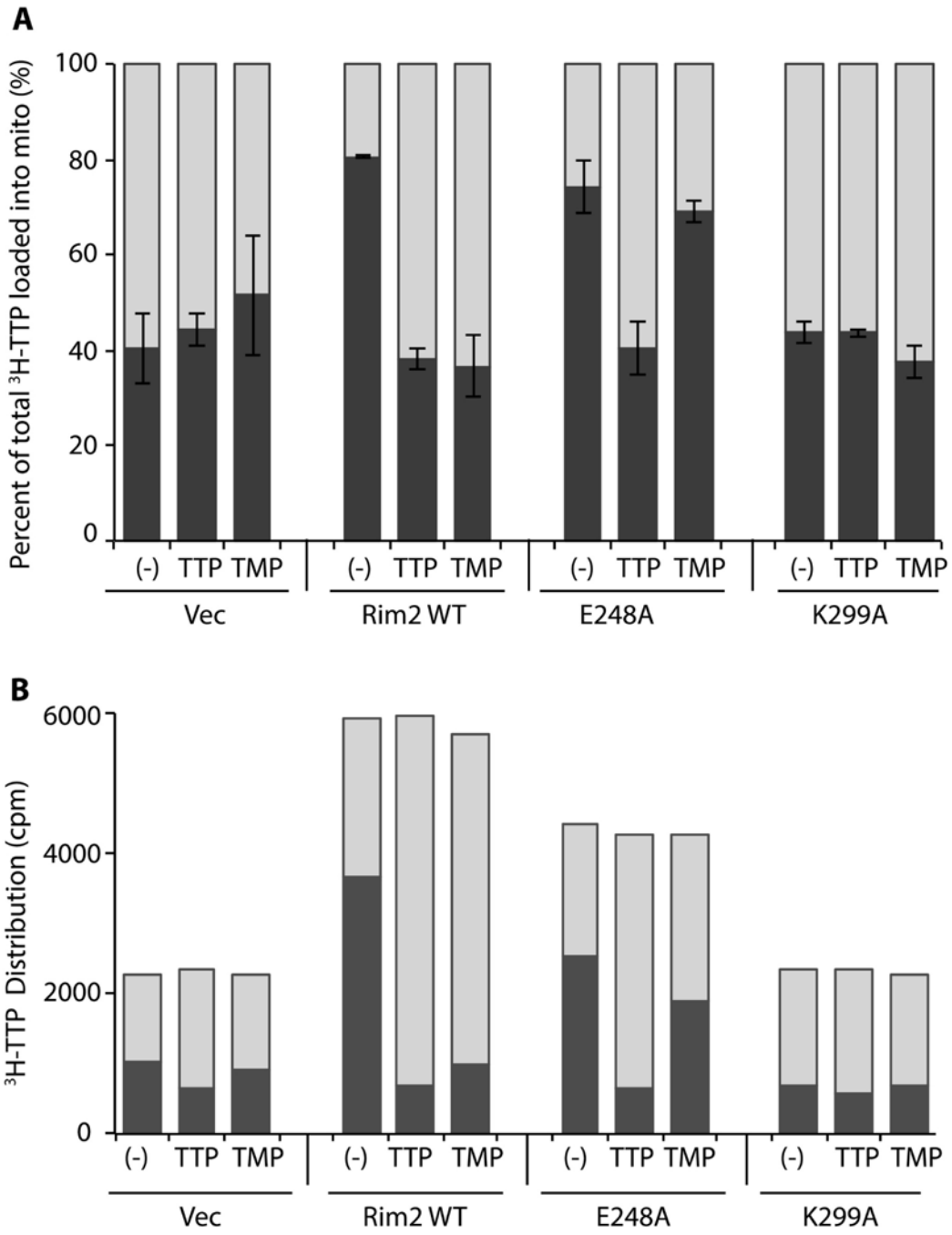

Fig. 5. Rim2 residue E248 is required for hetero but not homo exchange of pyrimidines.

Isolated mitochondria, from strain YS102–46 *(mrs3*Δ *mrs4*Δ *GAL-RIM2)* transformed with YEp351 (Vec), and YEp351 bearing: Rim2 (WT), Rim2 (E248A), Rim2 (K299A) and grown in the absence of galactose, were preloaded with ^{3}H-dTTP. The ^{3}H-dTTP was washed away and the mitochondria were resuspended in HS buffer containing 50 mM NaCl to which 100 μm TDP, 100 μM TTP or nothing (−) had been added. After 10 min incubation at room temperature, the mitochondria were pelleted and ^{3}H-TTP exported to the supernatant was quantified by liquid scintillation counting. (A) Results are expressed as a percentage of the

Author Manuscript Author Manuscript Author Manuscript Author Manuscript

total ^{3}H-TTP initially loaded into the mitochondria, with ^{3}H-dTTP remaining in mitochondria (dark gray) or ^{3}H-dTTP exchanged to supernatant (light gray). Error bars indicate SD (n=3). (B) A single typical exchange experiment is shown with results expressed as cpm ^{3}H-TTP retained in mitochondria (dark gray) or exported to the supernatant (light gray).

Author Manuscript Author Manuscript Author Manuscript Author Manuscript

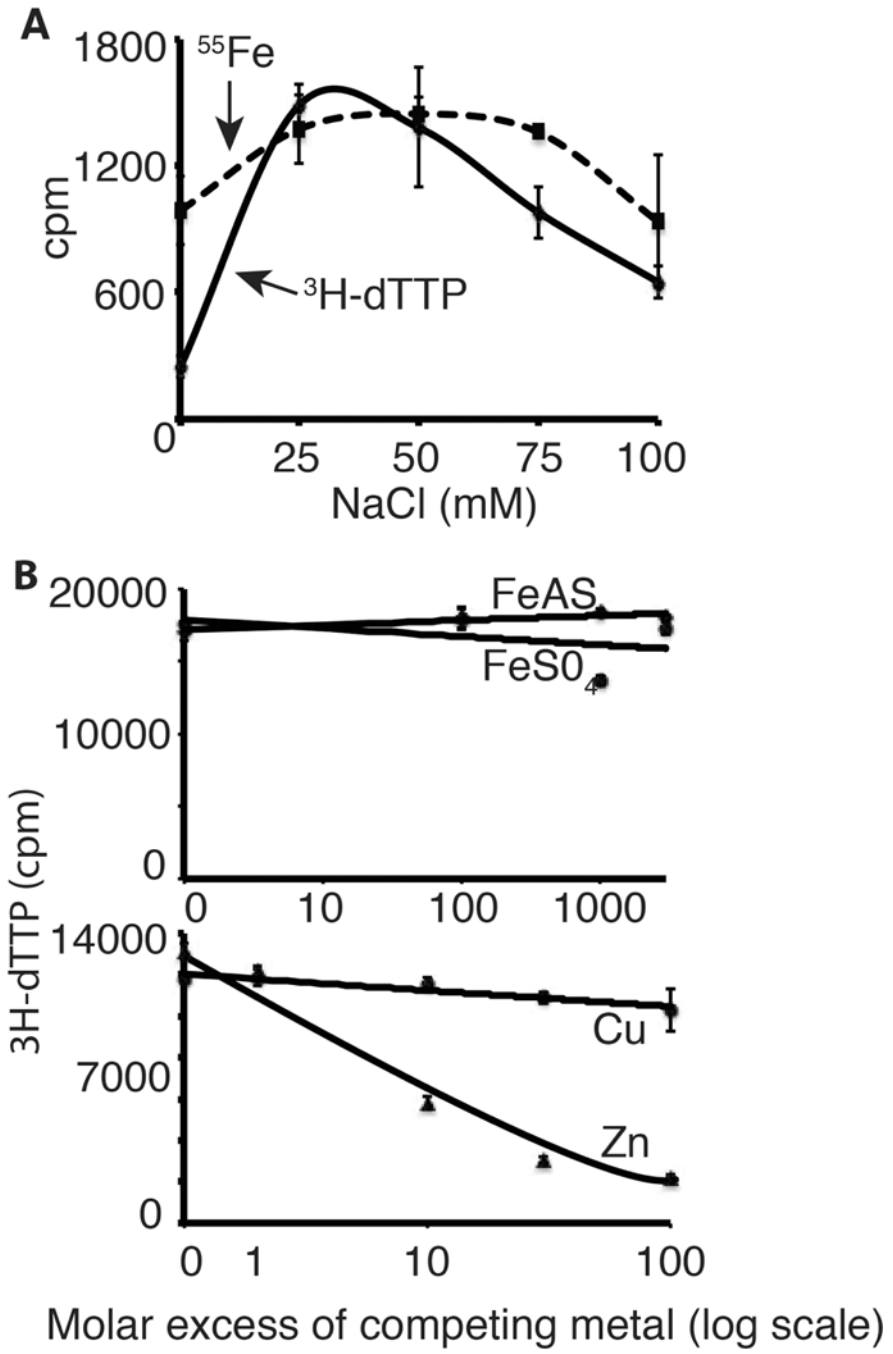

Fig. 6. Pyrimidine uptake is salt dependent and not competed by iron.

(A) Salt dependence: Mitochondria, from strain YS102–46 *(mrs3 mrs4 GAL-RIM2)* grown in the presence of galactose, were washed and resuspended in HS buffer with 0, 25, 50, 75, or 100 mM NaCl. They were then assayed for ^{3}H-dTTP uptake and ^{55}Fe incorporation into heme. Error bars indicate SD (n = 3). (B) Effect of metals: Isolated mitochondria from the same strain were preincubated with ferric ammonium sulfate, ferrous, zinc and copper sulfates at molar ratios to ^{3}H-dTTP ranging from 1:1 to 1: 3000. ^{3}H-dTTP was then added, and after 5 min incubation mitochondria were washed free of excess ^{3}H- dTTP, lysed, and

incorporated radioactivity was quantified by liquid scintillation counting. Experiments were performed in duplicate and error bars (where visible) represent the range of the duplicate values.

Author Manuscript Author Manuscript Author Manuscript Author Manuscript

Author Manuscript Author Manuscript Author Manuscript Author Manuscript

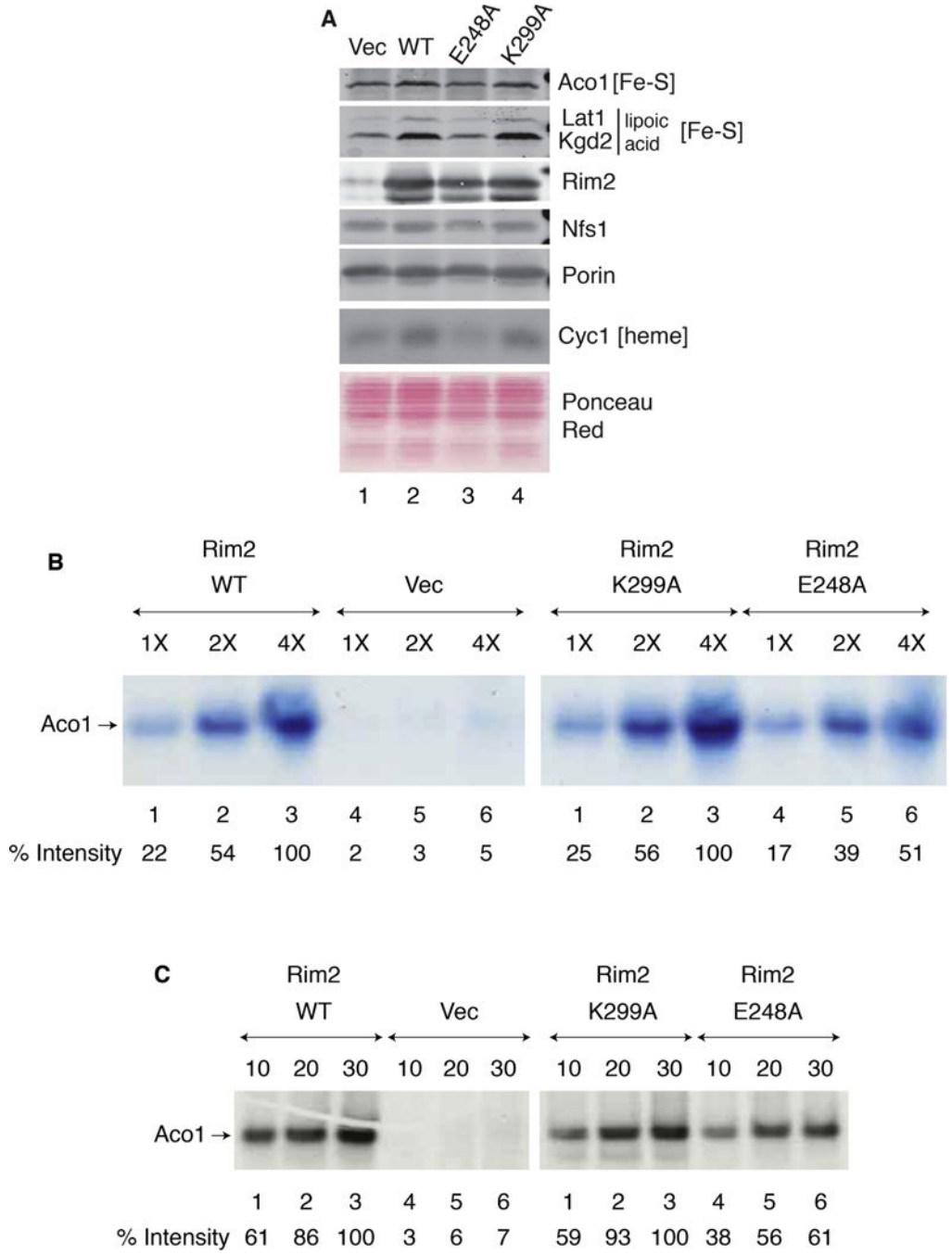

Fig. 7. Rim2 residue E248, but not K299, is essential for normal [Fe-S] cluster synthesis. Rim2 residue E248, but not K299, is essential for normal [Fe-S] cluster synthesis.

(A) Immunoblot analysis. Mitochondrial proteins (100 μg) from the indicated strains were separated by SDS-PAGE and transferred to nitrocellulose membranes. The membrane was stained with Ponceau S red and immunoblotted. Antibodies to the following proteins were used: aconitase Aco1, lipoamide-containing proteins Lat1 and Kgd2, cysteine desulfurase Nfs1, Porin, and cytochrome c Cyc1. Note that Lat1 encodes the dihydrolipoamide acetyl transferase component (E2) of the pyruvate dehydrogenase complex that catalyzes the oxidative decarboxylation of pyruvate to acetyl-Co. Kgd2 encodes the dihyrolipoamide

Author Manuscript Author Manuscript Author Manuscript Author Manuscript

transsuccinylase (E2) component of the alpha keto glutarate dehydrogenase complex, which catalyzes the oxidative decarboxylation of alpha-ketoglutarate to succinyl CoA. (B) In-gel aconitase activity assay. Isolated mitochondria from the indicated strains were lysed and proteins (1X = 50 μg) were separated by native gel electrophoresis and analyzed for aconitase activity using the in-gel assay. Left panel: Lanes 1–3 Rim2 WT, lanes 4–6 Vec. Right panel: lanes 1–3 Rim2 (K299A), lanes 4–6 Rim2 (E248A) (C) New Fe-S cluster synthesis: Transformants of strain YS102–46 (*GAL-RIM2* Δ*mrs3*/Δ*mrs4*) were grown in the absence of galactose, and mitochondria were isolated. The mitochondria were incubated with ferric ascorbate and ^{35}S-cysteine for 10, 20, and 30 min, followed by separation of the matrix fraction on a native gel. The labeled band, Aco1[Fe-^{35}S], represents newly formed Fe-S clusters on aconitase. Left panel: Lanes 1–3 Rim2 WT, lanes 4–6 Vec. Right panel: lanes 1–3 Rim2 (K299A), lanes 4–6 Rim2 (E248A).

Author Manuscript

Author Manuscript

Author Manuscript

Author Manuscript

Table 1.

Quantification of colonies shown in Fig 2 sectoring assay. Photographs in Fig 2 were from Expt 2.

Expt. 1						
Covering plasmid	**Vector**	**RIM2**	**K299A**	**E248A**	**MRS3**	**MRS4**
Red	61	8	43	47	1	2
Sectoring	0	12	5	0	23	17
White	0	20	12	0	42	28
Total	61	40	60	47	66	47
% White or sectoring	**0**	**80 %**	**28 %**	**0**	**98%**	**96 %**

Expt. 2						
Covering plasmid	**Vector**	**RIM2**	**K299A**	**E248A**	**MRS3**	**MRS4**
Red	170	122	168	249	48	49
Sectoring	0	44	12	0	73	48
White	0	24	15	0	46	43
Total	170	188	195	250	163	140
% White or sectoring	**0**	**36 %**	**14 %**	**0 %**	**73 %**	**65 %**